Micro-scale distillation – I: simulation

M. Fanelli, R. Arora, A. Glass, R. Litt, D. Qiu, L. Silva,
A. L. Tonkovich & D. Weidert
Velocys, Inc., USA

Abstract

Microchannel technology as applied to chemical processing has resulted in impressive improvements in performance thresholds. Studies published for more than a decade show that enhanced performance in chemical reactors can be largely attributed to the reduction of transport distances. Chemical distillation is now emerging as a new area for the application of microchannel technology.

A simplified method for simulating a microchannel distillation process has been developed and validated with experimental data. Both simulation and experiments show that the height of a theoretical transfer unit for the separation of hexane and cyclohexane in a microchannel distillation unit is reduced to centimetres. Vapour-side resistance was found to control mass transfer for the cases considered. The current simulation can serve as a tool for optimizing and refining the design of multiphase microchannel processes.
Keywords: distillation, simulation, separation, vapour-liquid, microchannel.

1 Introduction / background

Microchannel technology as applied to chemical processing has led to impressive improvements in performance thresholds. Several studies presented throughout the last decade show that reduction in transport distances significantly enhances the performance of chemical reactors. Reviews by Boger et al. [1], Hessel et al. [2], and Kreutzer et al. [3] provide excellent summaries of some of the key research and development efforts.

The Battelle Memorial Institute has conducted research in microchannel distillation since the early 2000s and holds U.S. and international patents in the field (Battelle [4–6]). A 2004 study by Wootton and deMello (Wootton [7])

WIT Transactions on Engineering Sciences, Vol 56, © 2007 WIT Press
www.witpress.com, ISSN 1743-3533 (on-line)
doi:10.2495/MPF070201

demonstrated continuous laminar microchannel evaporation of acetonitrile and dimethylformamide, adopting very small flow rates and co-current flows. The pioneering efforts reported in studies to date involved relatively small production quantities that are not directly applicable to industrial application. Our work is directed towards expanding microchannel distillation from the laboratory scale to the industrial scale.

Recognizing the potential for obtaining significant reduction in HETP (Height Equivalent to a Theoretical Plate) by microchannel distillation, a series of experiments and simulations was initiated to quantify the achievable enhancements. A representative laboratory distillation unit was built and distillation tests were run. The collected data were compared with the simulated results obtained with the Fluent™ Computational Fluid Dynamics (CFD) package. Comparative evaluations, adopting a binary hexane-cyclohexane system, have shown good order of magnitude correspondence between the model and experimental distillation trials. This information is now being used to refine and design alternate approaches to microchannel distillation for applications of industrial relevance.

2 Simulation methodology

The current simulation method allows relatively fast and direct estimation of distillation performance in a microchannel device. This method is not intended to be comprehensive. Its scope is to capture and model the primary phenomena that impact the distillation process with sufficient confidence for scoping analyses and future process refinement.

The present data manipulation involved the solution of species mass and momentum balances, but did not consider an energy balance or surface tension effects. Flow instability and heat transfer were not considered. The simulation was conducted under the following assumptions:

- a stationary interface, with no shear;
- interfacial concentrations based on ChemCAD provided distribution coefficients for each species, K_A, (linearly interpolated between the column extremes), such that

$$K_A = \frac{y_{Ai}}{x_{Ai}}, \tag{1}$$

  where y_{Ai} and x_{Ai} refer to the interfacial vapour and liquid compositions of species A, respectively;
- uni-directional equimolar counter-diffusion at the interface (Bird [8]), such that, within each phase, *j*,

$$N_{Aj} = -c_j D_{Aj} \left. \frac{dx_A}{dy} \right|_j, \tag{2}$$

where N_{Aj} is the molar flux of species A in the direction perpendicular to the interface, c_j is the molar density, D_{Aj} is the diffusivity of species A, and $\left.\frac{dx_A}{dy}\right|_j$ is the mole fraction gradient of species A in the direction perpendicular to the interface;

- equal molecular weight for the two species (an average of the actual molecular weights, given their similarity);
- constant fluid properties within each phase.

HETP estimates for each phase were calculated using the number of transfer units for that phase, n_j, and the length of the mass transfer channel, Z_{tot}, such that

$$n_j = \int_{x_{Ain\,j}}^{x_{Aout\,j}} \frac{dx_{Aj}}{x_{Ai\,j} - x_{Aj}} \qquad \text{and} \qquad HETP_j \sim \frac{Z_{tot}}{n_j} \tag{3}$$

where x_{Aj} is the cross-sectional area averaged concentration and $x_{Ai\,j}$ is the interfacial concentration along the channel, within each phase. Overall HETP's were estimated by combining the HETP for each phase; i.e.,

$$HETP_{total} = HETP_{vapor} + \frac{mG}{L} HETP_{liquid}, \tag{4}$$

where *m* is the slope of the equilibrium line (with the liquid mole fraction in the abscissa, the vapour mole fraction in the ordinate), and *G/L* is the ratio of the molar gas and liquid flow rates through the column (McCabe et al. [9]; Taylor and Krishna [10]).

The work was performed using the Fluent™ CFD package, currently used for some of our more intensive simulation work. Results were analyzed in terms of change in concentration profile along the channel axial length.

3 Experimental configuration and parameters

Experiments were performed using a stainless steel distillation unit involving counter-currently flowing vapour and liquid phase mixtures of hexane and cyclohexane. Liquid flowed vertically downward along a 178 μm deep stainless steel mesh. Vapour was fed to the device from a lower port, opposite the liquid outlet port. Liquid inlet and vapour outlet ports and vapour inlet and liquid outlet ports were slightly offset relative to each other, with the liquid ports lower than the vapour counterparts. Figure 1 shows representative schematics of the experimental setup, viewed from the top and side. The step in the cross section of the vapour channel, visible in the top view of the device, was a result of fabrication requirements.

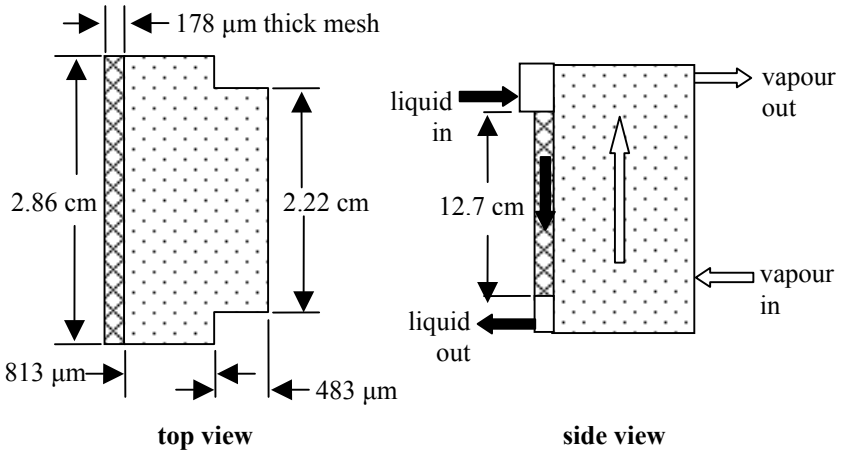

Figure 1: Representative schematics of the experimental distillation device.

Flow rates, feed concentrations and temperatures for the runs are summarized in Table 1. Testing was conducted at atmospheric pressure. The number of theoretical plates corresponding to the achieved separation were calculated using a rigorous ChemCAD distillation model with the liquid and vapour feeds input at the upper and lower plates, respectively.

Table 1: Relevant experimental run parameters.

	Case 1		Case 2	
Experimental Run Parameter	**Liquid**	**Vapour**	**Liquid**	**Vapour**
feed flow rate (liquid ml/min at ambient)	0.5	0.5	1.0	1.0
feed T (°C)	69	83	68	84
inlet hexane mole fraction	0.839	0.085	0.839	0.085

4 Simulated configuration and parameters

Two potential channel configurations were simulated to evaluate the sensitivity to different flow geometries.

1. The "mesh flow" configuration assumed the liquid flowed along the width of the channel wall as a continuous, uniform film with a depth equivalent to the 178 μm supporting mesh thickness and the uniform feed velocity that would result with the imposed volumetric feed rate.
2. The "falling film" configuration assumed the liquid flowed as a freely falling film along the width of the vertical wall, with the thickness and velocity dictated by the imposed volumetric feed rate. Calculations were based on the analysis of Bird et al. [8], according to which the liquid

Reynolds number corresponded to fully laminar flow, with no ripples. The shearing effect of the flowing vapour phase was assumed to be insignificant.

For each configuration, the section of the channel not filled with liquid was assumed to be filled with the counter-currently flowing vapour.

Physical properties were obtained from a ChemCAD distillation simulation of hexane-cyclohexane at the same temperature/pressure operating range as the experimental trials. Interfacial compositions were calculated from linear interpolation of the distribution coefficients between the column extremes. Material properties were assumed constant (averaged from the corresponding phase in the ChemCAD simulation); they are listed in Table 2. The feed compositions and representative flow rates for the simulations matched experimental values.

Table 2: Material properties and interfacial parameters used in the simulation. Gas and liquid diffusivities were estimated adopting standard methodologies (Poling et al. [11]).

Material Property	Liquid	Vapour
density (kg/m^3)	660	3.2
viscosity (kg/m.s)	3.0E-04	8.0E-06
diffusivity (m^2/s)	5.0E-09	4.5E-06
	Hexane	**cyclohexane**
molecular weight (g/mol)	85 (86 actual)	85 (84 actual)
distribution coefficients at the column top	0.79607	1.06210
distribution coefficients at the column bottom	0.94510	1.50565

The channel was assumed to be long and rectangular, and although the simulations were 3-dimensional, they were effectively run as 2-dimensional problems by defining the sidewalls as symmetric boundary conditions. The key parameters for the cases considered (named to correspond with the experimental runs) are listed in Table 3.

Table 3: Key run parameters for the simulated cases.

Case ID	Assumed Flow Type	Liquid Film Gap (μm)	Full Channel Flow Rate (liquid ml/min)	Liquid Velocity (m/s)	Vapour Velocity (m/s)
1a	falling film	36	0.5	0.0086	0.045
1b	mesh flow	178	0.5	0.0017	0.051
2a	falling film	43	1.0	0.0136	0.091
2b	mesh flow	178	1.0	0.0033	0.102

5 Results and discussion

Run results for the experimental and simulated cases are summarized in Table 4 and taken as key indicators of performance. As confirmed by the close correspondence of the experimental and simulated HETP's, the current simulation methodology can be deemed acceptable for predicting microchannel distillation performance.

Comparison of the simulated cases shows there is little impact of assumed liquid film gap on HETP, but the mesh flow assumption leads to:

- slightly better performance
- closer adhesion to experimental results.

Closer scrutiny of the concentration profiles for representative cases can shed light on these observations.

Table 4: Run results for the experimental and simulated cases.

Flow Rate (liquid ml/min)	Case ID	Description	HETP (cm) Liquid	Vapour	Overall
0.5	1	experiment	--	--	1.3
	1a	simulation - falling film	1.6	0.5	2.1
	1b	simulation - mesh flow	1.2	0.5	1.7
1.0	2	experiment	--	--	2.1
	2a	simulation - falling film	1.7	1.0	2.7
	2b	simulation - mesh flow	1.5	0.9	2.4

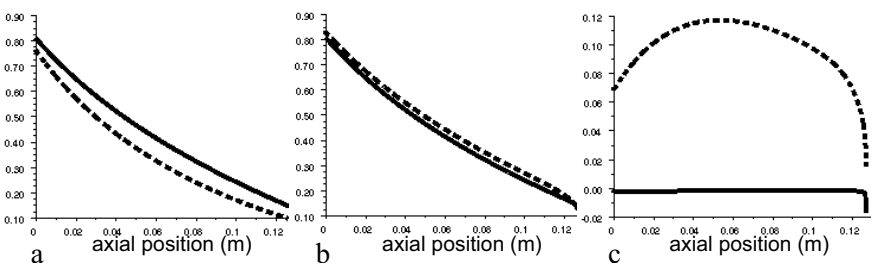

Figure 2: Representative hexane concentration profiles (mole fraction) as a function of axial position with respect to the channel top for simulated Case 1a (falling film). Dotted lines represent liquid-side, solid lines represent vapour-side profiles. Plot a presents interfacial concentrations, Plot b presents concentrations in the cells adjacent to the interface, Plot c shows the concentration difference driving the mass transfer at the interface (values in Plot b less values in Plot a).

Figure 2 shows three plots representing hexane concentration profiles for the low flow, falling film configuration:

a. at the interface,
b. in the cells adjacent to the interface,
c. as the difference between these values, representing the driving force for mass transfer along the channel length.

Figure 2c shows that for this case, as for all cases considered, the vapour layer near the interface equilibrates very quickly to the interfacial composition. Given the ease of this equilibration, the ability of the vapour species to diffuse through the vapour layer becomes the limiting phenomenon.

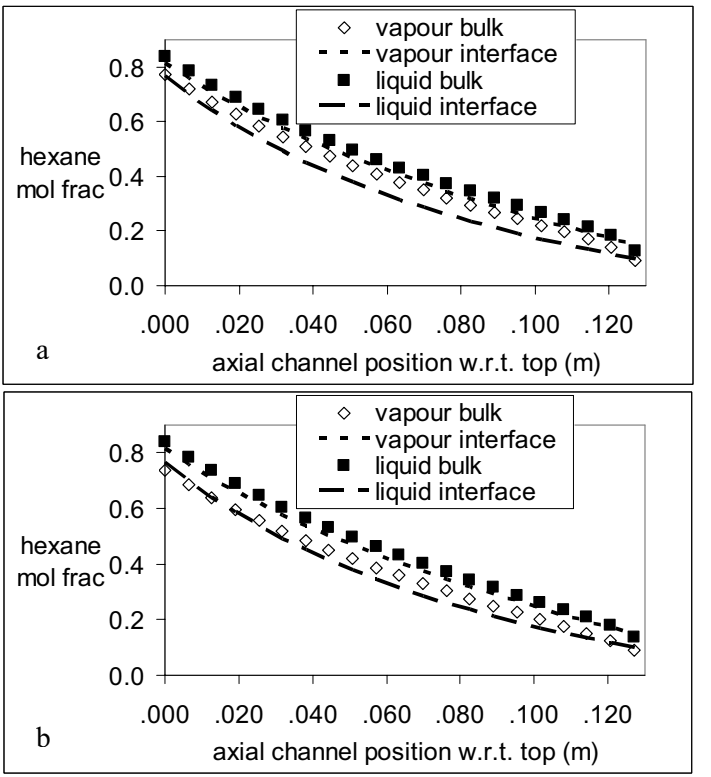

Figure 3: Representative surface area averaged concentration profiles and corresponding interfacial compositions for Cases 1a and 2a. Area averaged (bulk) concentration profiles were used to determine HETP values for each of the simulated runs.

The profiles in Figure 3 show the relative area averaged (bulk) concentrations along the length of the distillation unit for Cases 1a and 2a (these concentration differences were used to calculate HETP values for the simulated runs). Although comparison of the two plots shows no difference in liquid-side

concentration profiles, vapour-side concentration profiles show some dependence on flow velocity. At the higher flow rate, deviation between bulk and interfacial concentrations increased. Overall, since the vapour side controls mass transfer, the vapour-side HETP is more directly impacted by the change in flow rate.

6 Conclusion

A simulation approach has been successfully developed for simple and direct modelling of microchannel distillation processing using the Fluent™ CFD package. The methodology, which allows easy probing of different distillation geometries, was validated using a microchannel distillation device.

Experimental and simulated HETP's for the distillation of hexane from a hexane-cyclohexane mixture were found to be less than 3 cm. The mass transfer for the cases considered was found to be vapour-phase controlled. Additional comparative evaluations are ongoing to allow methodology refinement. The current approach can serve:

1. as a predictive tool,
2. as a means of investigating fundamental phenomena and their effect on multi-phase mass transfer performance.

Acknowledgements

The authors would like to acknowledge the Department of Energy for sponsoring this effort and the assistance of Fluent in troubleshooting the implementation of the simulation.

References

[1] Boger, T., Heibel, A.K., Sorensen, C.M., Monolithic catalysts for the chemical industry. *Industrial and Engineering Chemistry Research*, **43**, pp. 4602-4611, 2004.

[2] Hessel, V., Angeli, P., Gavriilidis, A., Lowe, H, Gas-liquid and gas-liquid-solid microstructured contacting principles and applications. *Industrial and Engineering Chemistry Research*, **44**, pp. 9750-9769, 2005.

[3] Kreutzer, M.T., Kapteijn, F., Moulijn, J.A., Heiszwolf, J.J., Multiphase monolith reactors: chemical reaction engineering of segmented flow in microchannels. *Chemical Engineering Science*, **60**, pp. 5895-5916, 2005.

[4] Battelle Memorial Institute, Improved Conditions for fluid separations in microchannels, capillary-driven fluid separations, and laminated devices capable of separating fluids. International Patent No. WO 03/049835 A1, 2003.

[5] Battelle Memorial Institute, Conditions for fluid separations in microchannels, capillary-driven fluid separations, and laminated devices capable of separating fluids. U.S. Patent No. 6,875,247 B2, 2005.

[6] Battelle Memorial Institute, Methods of contacting substances and microsystem contactors. U.S. Patent No. US 6,869,462 B2, 2005.
[7] Wootton, R.C.R., deMello, A.J., Continuous laminar evaporation: micron-scale distillation. *Chemical Communications*, pp. 266-267, 2004.
[8] Bird, R.B., Stewart, W.E., Lightfoot, E.N., *Transport Phenomena*, John Wiley & Sons: NY, 1960.
[9] McCabe, W.L., Smith, J.C., Harriott, P., *Unit Operations of Chemical Engineering*, 4th edition, McGraw-Hill Book Company: New York, 1985.
[10] Taylor, R., Krishna, R., *Multicomponent Mass Transfer*, John Wiley & Sons: New York, 1993.
[11] Poling, B.E., Prausnitz, J.M., O'Connell, J.P., *The Properties of Gases and Liquids*, 5th ed., McGraw-Hill Book Company: New York, 2001.